

A model for the decay of a wall shock in a large abrupt area change

By S. A. SLOAN AND M. A. NETTLETON

Central Electricity Research Laboratories, Kelvin Avenue,
Leatherhead, Surrey KT22 7SE, England

(Received 5 March 1977 and in revised form 28 March 1978)

A series of initially planar shock waves was allowed to expand from a shock tube into a near half-space. The strength of the wall shock was measured at two positions on the slightly concave front wall. These measurements are compared with shock strengths predicted by a shock-dynamic model based on the cylindrical expansion of a critical shock. Chisnell's (1957) theory is used to account for the effect of the increasing surface area of the expanding wall shock, and Whitham's (1957) treatment to correct for the curvature of the wall. The critical shock strength is obtained from Skews' (1967) experimental measurements of the Mach number of the self-similar wall shock following two-dimensional diffraction at a 90° edge.

The model predicts the relatively small degree of attenuation observed between the measuring stations, but overestimates the absolute shock strength. The most likely cause is that, in the early stages of expansion, the wall shock experiences further attenuation owing to its interaction with the expanding flow. These effects are shown to be short range and of negligible importance at the first measuring station, 1.86 tube diameters from the axis. Thus, using the experimental results at this station as the starting point, the model predicts accurately the shock strength at 3.76 diameters. It is concluded that Chisnell's theory can be applied to the weakening of the wall shock in ducts with large abrupt changes in cross-section only when the wall shock is some distance from the entrance to the area change.

1. Introduction

The behaviour of shock waves in complex configurations is of practical concern in the estimation of impulsive loading during dust or gas explosions. Waves of low strength are of interest to the designers of internal combustion engines. Apart from the practical aspects, there is still need of a better understanding of the interactions of shock waves in ducts of varying cross-section.

Chester (1953, 1954) developed an analytical treatment for the motion of a shock wave through a gradually diverging duct. This linearization is strictly valid only for small area changes. Chisnell (1957) integrated Chester's equations and derived a relationship connecting the local properties of the shock wave and the cross-sectional area of the duct A which is most simply stated as

$$Af(Z) = \text{constant}, \quad (1)$$

where $f(Z)$ is a known function of the shock strength (or pressure ratio Z) and the ratio of specific heats γ .

Chisnell's equation has been used in most calculations of shock wave interactions in ducts with either sudden or gradual area changes. Indeed it is basic to Whitham's (1957, 1959) more general theory of shock dynamics. However the theoretical results have not always agreed well with experimental measurements.

Davies & Guy (1971) compared experimental and theoretical results for 4:1 and 10:1 expansions and found a satisfactory correlation only for the smaller area change. Deckker & Gururaja (1970) examined the decay of a shock wave in diffusers with semi-divergence angles of from 10° to 90° and found that the model overestimated the degree of attenuation for all but the very weakest shocks. Further, the predicted shock strength at the exit of the diffuser was much greater than the pressure measured 'a suitable distance behind the transmitted wave'. Conversely, in similar experiments, Nettleton (1973) found adequate correlation for shocks with M up to 3.0 at 5 diameters downstream of diffusers for area ratios up to 5.0 and semi-divergence angles up to 15° . Thus the general application of Chisnell's equation remains a matter of controversy. One of the problems is that the predictions are compared with inappropriate parameters; for instance, the strength of the unsteady shock has been characterized by a single measurement at the divergent wall of an expansion duct. Dekker & Gururaja (1970) compared the results of applying Chisnell's theory with pressures measured 'a suitable distance behind the transmitted wave' at 40 diameters from the exit plane. Here the flow must be approaching a steady state, a condition with which Chisnell's theory is unlikely to correlate. Further, measurements outside the area change, even if made close to the exit, may be misleading, since they could be affected by the shock wave reflected as the transmitted wave enters the exit duct. Only measurements made within the area change should be compared with predictions from shock-dynamic models.

There exists a certain ambiguity about the interpretation of the shock strength obtained from (1). The strength of a shock wave in an area change is non-uniform, but can be assigned an average value, predicted by Chisnell's theory. In a situation where the strength varies rapidly along the shock front, this bears little relevance to the true unsteady shock strength at a given point on the front. The average value approximates to the unsteady strength only when applied to a portion of the shock front across which the strength is not changing rapidly.

In order to overcome these difficulties in a study of the axial decay of an expanding shock, the authors (1975) formulated the area relationships in terms of the ratio of the surface area of an axial element of the decaying shock wave to that of the corresponding element of the critical shock. The critical shock is the configuration at the instant of axial decay. The predictions of this model were in excellent agreement with the experimental measurements of axial shock strengths in large abrupt area changes where the shock was free to expand in either two or three dimensions. It was concluded that Chisnell's theory could be extended to analyse the shock strengths at the axis of large abrupt area changes, provided that the initial area was defined in terms of the surface area of the axial segment of the critical shock.

The complementary results reported in this paper are for shock waves decaying along the slightly concave front wall of the same three-dimensional abrupt area change. An idealized model is developed in §4 in which the concept of the critical shock is

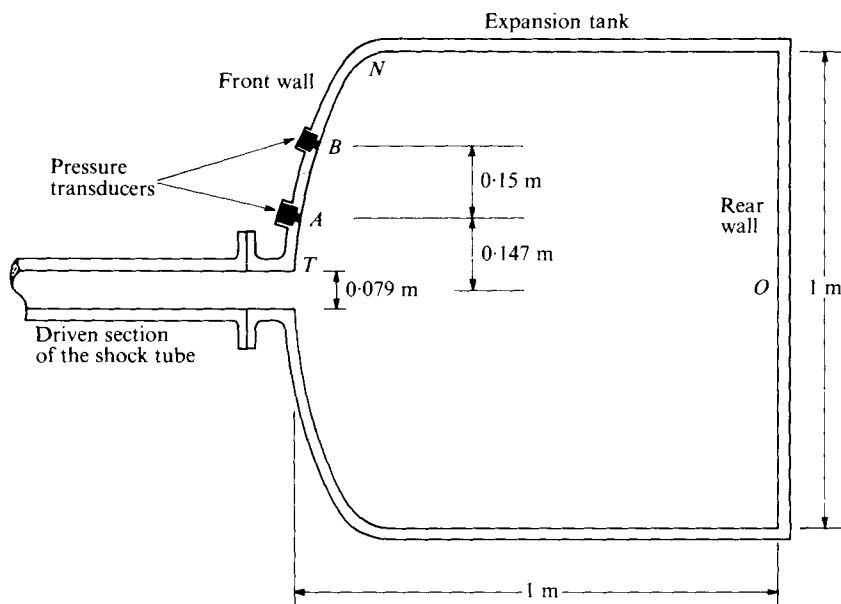


FIGURE 1. Shock tube and expansion tank.

combined with Skews' experimental measurements of the self-similar wall shock following diffraction at a 90° edge. The attenuation due to the cylindrically symmetrical expansion of the wall shock is quantified by application of Chisnell's equations, and Whitham's treatment is used to correct for the curvature of the wall. This is shown to be realistic, although it considerably overestimates the strength of the wall shock. The model combines several theories, but it is essentially a test of Chisnell's theory. Discrepancies between the predicted and experimental results are explained by the further attenuation of the wall shock owing to its interaction with the rapidly expanding pursuing flow.

2. Experimental

Figure 1 is a scale diagram of the near half-space formed by the expansion tank (1 m in diameter and 1 m long) attached to the driven section of a 79 mm bore shock tube. The front wall of the tank is a section of radius 1 m centred on the axis of the tube at O . Hence the angle θ_w between the normal to the wall and the axis of the shock tube is 8.5° at A and 17.3° at B , these points being at radial distances of 0.147 m and 0.297 m respectively. The Mach number of the initial shock was calculated at the entrance of the tank, which was taken as the sharp edge T where the rapid area change begins. The lead-in duct to the tank is of the same bore and co-axial with the shock tube. The angle between the tangent to the wall at T and the axis of the tube is 87.8° .

Planar shocks of initial Mach number between 1.5 and 3.5 were allowed to expand into the tank. The passage of the shock wave radially along the curved wall was recorded by Kistler 601 A pressure transducers mounted flush with the wall at A and B .

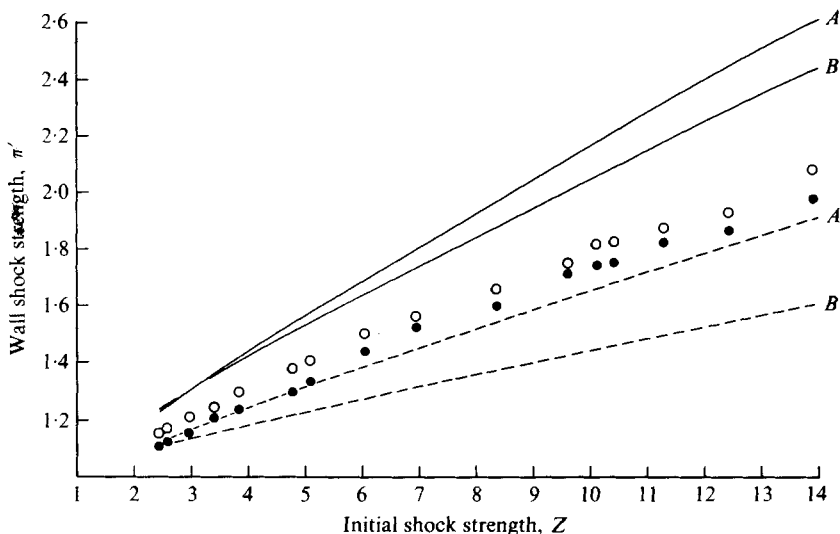


FIGURE 3. Experimental wall shock strength and predictions of the critical shock model. ○, ●, experimental at *A* and *B*; —, ---, model predictions for cylindrical or spherical symmetry.

Pressure profiles such as figure 2 (plate 1) were obtained from each transducer on separate dual-beam oscilloscopes at 1 ms cm^{-1} . By means of an internal sweep delay, peak (*a*), due to the passage of the wall shock, was also displayed at $20 \mu\text{s cm}^{-1}$. Summation of the sweep delay and the time on the trace before the arrival of the wall shock gave the time τ for the shock to arrive at the appropriate gauge.

3. Results

The pressure profiles at stations *A* and *B* shown in figure 2 are typical. The wave processes involved have been discussed by Smith (1966). The transducer first experiences an increase in pressure at (*a*) due to the passage of the wall shock across the gauge. This is followed by a strong expansion wave which lowers the pressure at (*b*) below the initial pressure P_1 as the gas behind the initial shock expands into the tank. The peaks at (*c*) are attributed to weak reflexions as the wall shock turns the sharp bend at *N* (figure 1). They are noticeably more intense at station *A* because of the strengthening effect of the concave front wall and the focusing of the radially converging waves. The largest peaks (*d*) are due to the arrival of the shock wave reflected from the rear wall of the tank.

The present quantitative analysis concerns only peak (*a*). Figure 3 shows the near linear dependence on Z of the wall shock strengths π'_A and π'_B recorded at stations *A* and *B*. The difference between the measurements at the two stations increases only slightly with Z ; π'_A is always slightly greater than π'_B . This is a genuine difference and not due to calibration errors, since interchanging the transducers has no significant effect. The wall shock has attenuated greatly from the initial shock strength, so that the over-pressure $\pi' - 1$ at each station is generally less than 10% of the initial over-pressure $Z - 1$. Thus most of the decay in shock strength occurs before the shock wave

Initial shock strength Z	Shock strength		Axial distance X_A (m)	Shock strength		Axial distance X_B (m)
	Wall A	Axial		Wall B	Axial	
2.64	1.18	1.51	0.144	1.12	1.10	0.304
4.13	1.33	1.93	0.156	1.27	1.40	0.324
5.18	1.42	2.20	0.163	1.36	1.56	0.337
6.78	1.55	2.58	0.173	1.49	1.73	0.352

TABLE 1. Comparison of simultaneous wall and axial shock strengths.

arrives at A , with only a slight further attenuation between A and B . (The curves in figure 3 arise from the model developed in § 4.)

The present results provide the strength of the wall shock at A and B , together with the time τ taken to travel from the entrance of the tank. Similar measurements have been reported (Sloan & Nettleton 1975) of the axial decay of shocks with four different initial strengths. These results are combined in table 1 to give the axial shock strength and position at the instant of the wall shock measurement. While the axial shock travels the distances X_A and X_B , the wall shock propagates 0.108 and 0.258 m from the edge of the shock tube along the concave wall to stations A and B respectively. It is obvious that the axial shock is stronger and travels further in equal intervals of time.

4. The wall shock

4.1. General

The wall shock is produced by a combination of hydrodynamic processes originating at the entrance of the abrupt area change. The initial shock wave undergoes diffraction at the sharp edge T before expanding axially along the wall. This wall shock is subject to the following simultaneous interactions.

- (i) Attenuation due to the increase in surface area of the expanding shock wave.
- (ii) Attenuation due to the effect of the rapidly expanding flow in the gas behind the wall shock.
- (iii) Enhancement due to the concave curvature of the wall.

The theories of Chisnell (1957) and Whitham (1957, 1959) are used to model (i) and (iii). It is assumed that the interaction of the wall shock with the pursuing flow is negligible.

4.2. A critical shock model

The authors (1975) developed the concept of the critical shock to analyse experimental measurements of axial shock strengths. Basically the analysis requires that the Chisnell relationship is applied only when the expansion process predominates over other wave processes, such as diffraction and reflexion, and only to a shock front for which the average strength approximates to the true shock strength. Application to the present results requires a closer examination of the diffraction process.

Consider now a planar shock wave diffracting around a 90° sharp corner T , where the shock is free to expand only in the x, y plane. Figure 4 represents successive

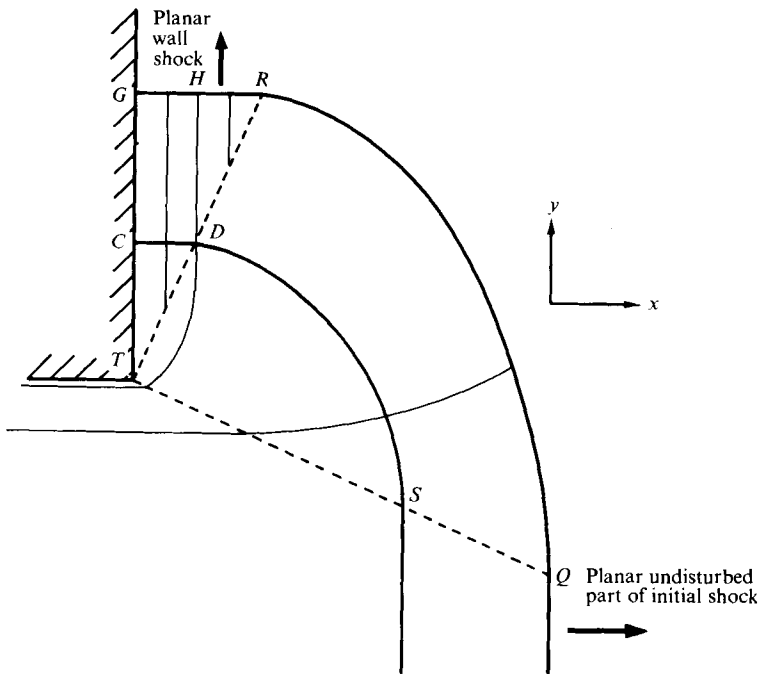


FIGURE 4. Successive positions of a shock wave diffracting in two dimensions. —, shock wave; ---, expansion fan; —, ray.

positions of the wave pattern for an idealized case. The head of the expansion wave, which propagates from the corner with sonic velocity relative to the shocked gas, overtakes the shock wave along the straight line TS . The strength of the shock front decreases along the shock envelope from S to D , where it meets the tail of the expansion wave. The strength of the shock at D is that of the wall shock CD , which is tangential to the curved shock envelope and normal to the wall. Whitham's idealized treatment requires that this configuration is self-similar. Thus for a given initial Mach number, an increase in time simply increases the scale of the diffraction SDC to QRG . In particular, the wall shock has constant velocity and thus constant strength Z_w .

Whitham defined a ray to be orthogonal to the shock at the point of contact. Since in the idealized treatment the planar wall shock remains normal to the wall, the rays connecting two successive positions of the wall shock are parallel in the region TRG . (In figure 4 only sample rays are extended into the region TRQ , where the rays are curved.) As the diffraction pattern expands, the point D moves away from the wall along the straight line TDR as more of the shock envelope decays to the strength of the wall shock. Thus effectively there is no expansion of the initially formed wall shock in the x direction, only a decay of the shock envelope to the strength Z_w of the self-similar wall shock.

In order to model a three-dimensional diffraction, it is assumed, by analogy, that the wall shock remains normal to the wall but is free to expand only in the plane y, z of the wall. Thus as the shock propagates along the wall, it undergoes continuous attenuation owing to its increasing surface area.

Figure 5 represents a cross-section through two positions of an expanding shock wave bounded by a planar wall. The shaded areas $CDEF$ and $GHJK$ are sections of

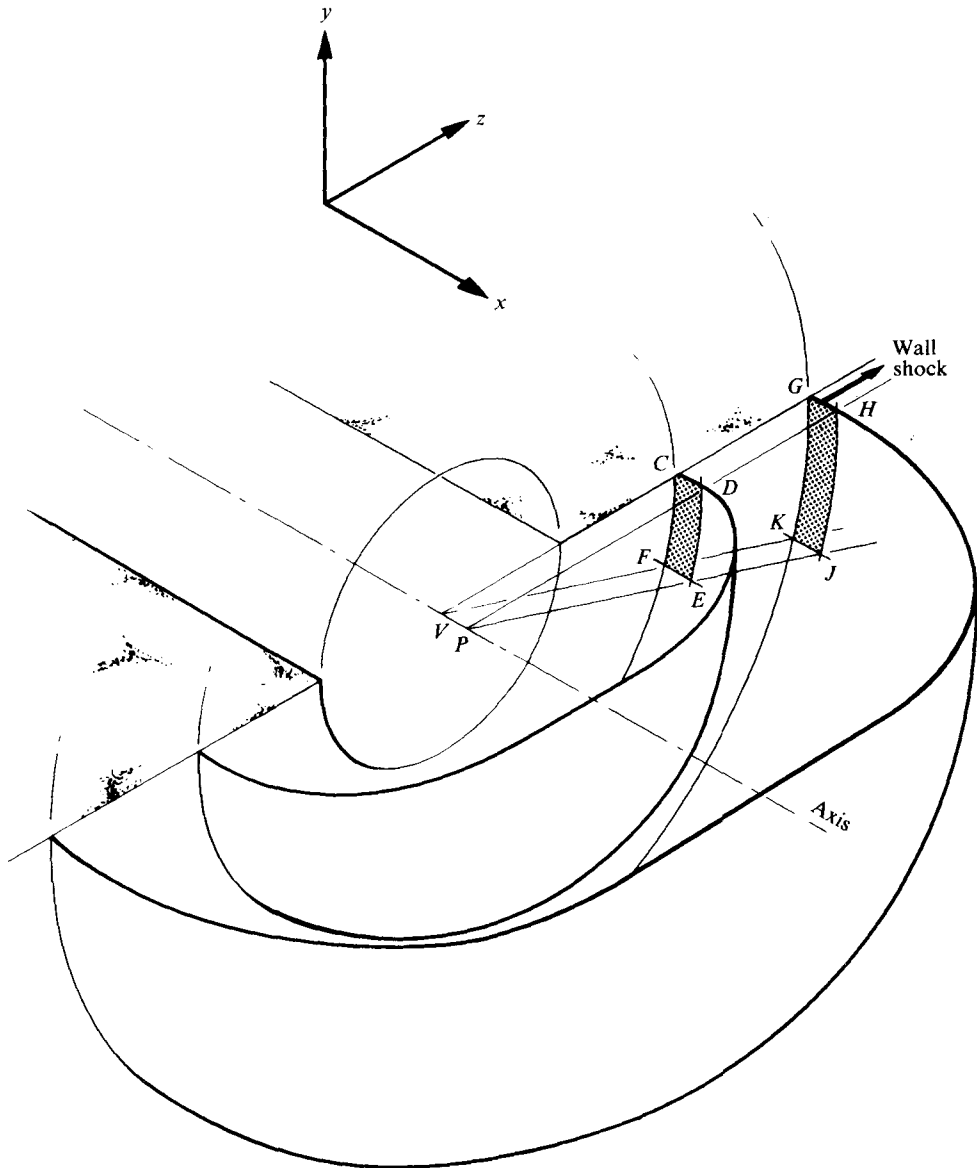


FIGURE 5. Section through successive positions of a shock wave expanding in three dimensions.

the wall shock which must be cylindrical about the axis, since the model constrains the wall shock to expand only in the y, z plane and the system is axisymmetric. Furthermore, since rays are by definition normal to the shock, the common radii VG, VK and PH, PJ can be considered as boundaries of a hypothetical ray tube. The propagation of an element of a shock wave along a ray tube is analogous to propagation in a tube of smoothly varying cross-section with solid walls. Thus the shaded section $CDEF$ of the wall shock expands to $GHJK$, and owing to the cylindrical symmetry of the wall shock, the ratio of the surface areas is equal to the ratio of the radii.

Extrapolation of the model towards the instant of diffraction implies that the wall shock tends to the strength Z_w in the self-similar case of two-dimensional diffraction. In the limit this is the critical shock and is the initial configuration for the present model of the expanding wall shock. This system fulfils the requirements of the critical shock model; that is, provided that there is negligible interaction between the expanding shock wave and the pursuing flow, the predominant influence is the change in surface area due to the local geometry, as defined by the ray tubes. Further, the wall shock is of uniform strength up to the point D , where it merges with the envelope of the main shock.

The surface area A' of the expanding shock wave is defined as the area of the cylindrical shock wave in a given ray tube adjacent to the wall, such as GVK , HPJ . The surface area A_w of the critical shock is the limit of this area as the segment of the shock is extrapolated backwards to the instant of diffraction of the initial shock. Clearly A_w is proportional to r_0 , the radius of the throat of the area change.

Consider now an abrupt area change with a planar side wall normal to the axis. In the idealized model the shock wave is diffracted at the edge, instantly becoming the critical shock of strength Z_w and surface area A_w proportional to the radius of the exit duct. The subsequent expansion to a strength Z' has cylindrical symmetry. For the first step of a computation of shock attenuation,

$$\frac{A'}{A_w} = \frac{r}{r_0} = \frac{f(Z_w)}{f(Z')}, \quad (2)$$

where r is the distance of the wall shock from the axis and $f(Z)$ is the appropriate Chisnell function [see (1)]. For subsequent steps,

$$\frac{A'_{n+1}}{A'_n} = \frac{r_{n+1}}{r_n} = \frac{f(Z'_n)}{f(Z'_{n+1})}. \quad (3)$$

These relationships for a planar wall are additive and the result is identical whether it is computed in a series of small steps or a single step.

The effect on the shock strength of introducing wall curvature into the calculation is computed as a series of small perturbations on the planar-wall solution. Since the expansion of the shock and its strengthening occur simultaneously, it is not sufficient to predict the shock strength Z' on a planar wall and correct this for the curvature to obtain the strength π' on a curved wall. The results are not additive, so that the correction must be carried out in a number of small steps. Essentially the curved wall is replaced by a series of small straight tangential wedges.

Consider now a plane shock moving from a planar to a curved wall. By Whitham's theory, the solution is a simple wave through which ω' , corresponding to the new shock strength, is given by

$$\omega' = \omega + \theta_w, \quad (4)$$

where θ_w , measured in radians, is the change in direction of the normal to the wall and is positive for a concave wall, negative for a convex wall. In the present experiments θ_w is 0.148 and 0.302 at A and B respectively.

For a wall of radius of curvature R , the distance measured along the wall between the wall shock and the axis is $R\theta_w$. This replaces r in (2) and (3). The computational

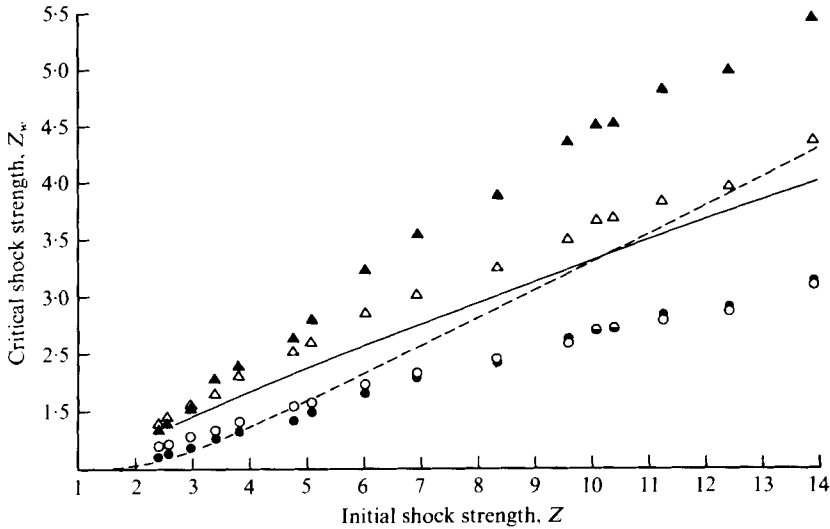


FIGURE 6. The strength of the critical shock. \circ , \bullet , derived from π'_A and π'_B , cylindrical symmetry; Δ , \blacktriangle , derived from π'_A and π'_B , spherical symmetry; —, Skews; ---, Whitham.

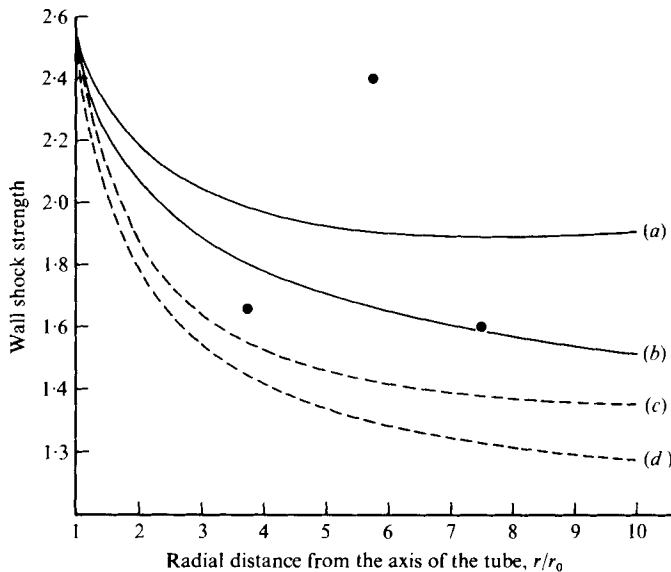


FIGURE 7. Decay of a shock wave of initial strength 8.35. (a) π' (concave wall), cylindrical symmetry. (b) Z' (planar wall), cylindrical symmetry. (c) π' (concave wall), spherical symmetry. (d) Z' (planar wall), spherical symmetry. \bullet , experimental.

procedure was to build up to the required values of θ_w in small increments, and after each step to use (4) to correct for the curvature. This provided a new (known) value of the shock strength Z' and thus the value of the Chisnell function at the start of the next step of the computation. The convergence tests were that there was a negligible change in π' at any point on the wall when the increment was greatly reduced and that the result was unaffected when the curvature correction was performed before the

expansion step. An increment of 0.0175 (1°) proved satisfactory in the present case. Reducing this by a factor of 10 changed the resultant values of π' by much less than 1%.

A simultaneous numerical integration of (1) and (4) gave identical results to this small-step procedure. However the former proved to be a more cumbersome computation and was used only to confirm the small-step calculations at several initial shock strengths.

The predictions of the model are presented for the passage of the wall shock across either a curved (π') or a planar (Z') wall. To demonstrate the sensitivity of the model, the results for the cylindrically expanding wall shock are also compared with those where the critical diffracted shock was assumed to have expanded with spherical symmetry.

4.3. *The strength of the critical shock*

Theoretically the critical shock strength at the instant of diffraction must be the same in two and three dimensions. Locally the fluid does not know about the existence of axisymmetry at that instant and becomes aware of it only as the waves spread out. This is independent of any particular model. Thus although the shock wave is free to expand in three dimensions, the strength of the critical shock is the same as that of the self-similar two-dimensional diffracted wall shock (Z_w).

This can be obtained directly by Whitham's theory with $\theta_w = -1.53$ (87.8°) in (4). However the theory is known to be inadequate for weak shocks leading to negative values of ω' , i.e. for $Z < 1.78$. Physically this means that diffraction of these weak shocks results in sound waves. This does not agree with Skews' (1967) experiments, in which shocks of significant strength were measured for weak initial shocks. Skews' results for two-dimensional diffraction at a 90° edge provide more satisfactory values for Z_w and consequently are used in the quantitative application of the model. These have been corrected by use of (2) to give values for an 87.8° ($\theta_w = +0.039$) edge and are plotted in figure 6 together with those from Whitham's theory.

4.4. *Comparison between the model and experimental results*

A typical initial shock of Mach number 2.7 ($Z = 8.35$) in air produces a critical shock strength Z_w of 2.53. Figure 7 illustrates the effect of the curvature of the wall and also demonstrates the sensitivity of the model to the symmetry of the expanding shock. The degree of amplification of the wall shock due to the curvature of the wall is most pronounced for the cylindrically expanding shock, because the degree of shock strengthening is independent of the assumed symmetry and is proportionately greater for stronger shocks. The model shows that, after an initial period of decay, the strengthening effect of the curvature eventually predominates over the attenuation due to expansion and the wall shock wave increases in strength. For a side wall with a smaller radius of curvature, or for a weaker initial shock, this effect is accentuated and occurs nearer to the entrance of the area change. Although shock strengthening has not been observed in the present experiments, it seems likely that it could occur under the appropriate conditions.

Quantitatively the correlation between the predictions of the model and the experimental results is poor. The measured shock strengths (figure 7) lie between the computations for the two assumed symmetries. This is generally true as illustrated

in figure 3, where the predicted values of π' are compared with the experimental measurements over the complete range of initial shock strengths.

For a wall shock assumed to be expanding with cylindrical symmetry the model predicts reasonably well the attenuation between stations A and B , except for very weak initial shock strengths, when it predicts shock strengthening between A and B for $Z < 2.8$. This was not observed in practice but is readily explained by the tendency of Whitham's theory to over-correct for the curvature. Quantitatively, the model overestimates the strength of the shock by 25% and 10% respectively for strong and weak initial shocks.

When the expansion is assumed to have spherical symmetry, the model greatly overestimates the attenuation between stations A and B , but never predicts shock strengthening. The computed shocks are always weaker than those measured experimentally.

5. Discussion

The essential feature of the experimental results is the small degree of attenuation of the wall shock between stations A and B . This is reasonably predicted by the model, but the absolute strength of the wall shock is considerably overestimated. Thus the basic assumptions of the model require examination.

The premise of cylindrical symmetry has been discussed and is apparently sound. There remain the assumptions of the strength of the critical shock and negligible interaction between the expanding flow and the decaying shock, so that attenuation is due solely to the increasing surface area of the shock. These related assumptions have been examined by the following procedure. On the premise of cylindrical symmetry, the model was extrapolated backwards to the instant of diffraction to determine the actual critical shock strength required to give the experimental results. For each initial shock strength, the measurements of π' at A and B each predicted a value of the strength of the critical shock. If the model is valid, then these should be coincident.

Figure 6 is a plot of these derived critical shock strengths over a range of Z . It can be seen that when cylindrical expansion is assumed the pairs of critical shock strength values are effectively coincident for $Z > 7.0$. For weaker shocks the values diverge by about 0.1, and the critical shock strength derived from π'_A is always greater than that derived from π'_B . This is partly accounted for by the inadequacy of Whitham's theory when applied to weak shocks; this theory tends to concentrate the curvature of the wall over an insufficiently large segment of the shock wave, leading to an overestimation of the relative shock strengthening on a concave wall. Consequently each of the predicted critical shock strengths for $Z < 7.0$ is too low, and the error is greater for the results from station B . Correction of this would bring the derived critical shock strengths nearer to the coincidence required by the idealized model.

The argument that the degree of attenuation observed between A and B is so small that it is insensitive to the choice of model is disproved by repetition of the above procedure for a critical shock expanding with spherical symmetry. The derived critical shock strengths now do not show any tendency to coincide, except for very low initial shock strengths.

This is strong evidence that the model is essentially valid. An important feature of figure 6 is that the derived strength of the critical shock is lower than that of Skews'

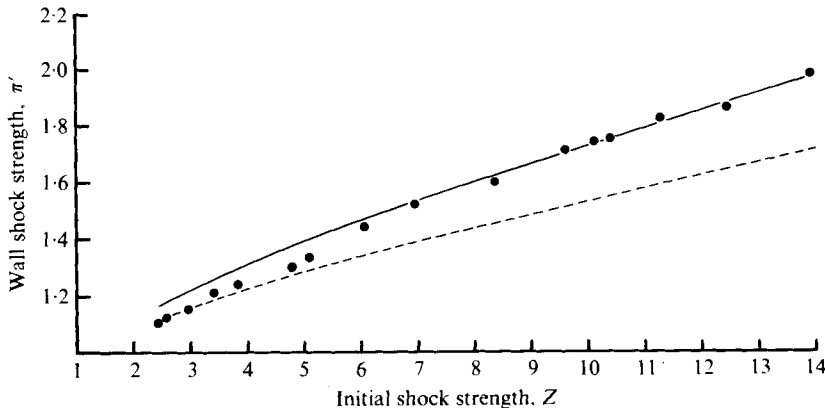


FIGURE 8. Wall shock strength at B . —, cylindrical expansion; ---, spherical expansion; ●, experimental.

self-similar diffracted shock for all initial shock strengths. Thus the self-similar shock wave must experience further attenuation, which may occur either at the instant of diffraction or soon after. Thus there may be a fundamental, unappreciated difference between the diffraction processes in two and three dimensions, and therefore the assumptions as to the strength of the critical shock are wrong. Alternatively, the interaction between the expanding shock wave and the unsteady pursuing flow may not be negligible, as assumed in the model. This seems a more probable cause of the observed discrepancies, which are believed to be evidence of the considerable influence of these interactions in the present experiments.

The near-coincidence of the strengths of the critical shock derived from the pairs of experimental measurements of π' suggests that this further attenuation must occur soon after diffraction and that the assumption of negligible interaction with the flow becomes increasingly valid as the wall shock moves away from the entrance to the area change. Consequently a more accurate assessment of the strength of the decaying wall shock should be obtained by starting the computation at A and using the experimental values π'_A of the wall shock strength. In the model these were allowed to expand to station B with either cylindrical or spherical symmetry. With $Z > 7.0$, the predictions for cylindrical symmetry are within 2% of the measured values. For weaker initial shocks the correlation deteriorates to 5%. Nevertheless, this is a very satisfactory result and together with figure 6 is strong evidence that the wall shock is appropriately modelled by cylindrical symmetry and that the Chisnell-Whitham approach can be applied to ducts with large abrupt increases in cross-section only when the wall shock is some distance from the entrance to the area change. Starting the model at the instant of diffraction leads to an overestimation of the wall shock strength, as already discussed. Clearly, allowing the shock to expand with spherical symmetry between stations A and B (figure 8) leads to much weaker wall shocks than those measured, again demonstrating the sensitivity of the model.

Previous work (Sloan & Nettleton 1975) introducing the concept of the critical shock concluded that the model provided only a method of analysis and a means of extrapolating beyond the conditions of experiments. Direct prediction of the axial shock strength was not possible because the centre of symmetry of the expanding

shock wave had to be determined by experiment. In theory the present model should provide absolute values, because the value Z_w of the self-similar wall shock is known and the centre of symmetry must be the axis. Unfortunately it has been shown that the expanding shock wave experiences further attenuation owing to interactions between the characteristics generated by the expanding shock and the unsteady flow behind it. This limits the accuracy of the model.

6. Conclusions

A model of the behaviour of a wall shock in a large abrupt area expansion has been developed on the basis of cylindrical expansion of the initial diffracted shock (Skews 1967). The attenuation of the shock wave is described by Chisnell's (1957) theory, and Whitham's (1957) treatment accounts for the strengthening along the concave wall.

The experimental observation that the shock wave at the wall experiences only a small degree of attenuation between the two measuring stations, 1.86 and 3.76 tube diameters from the axis, is shown to arise because of the constraint of cylindrically symmetrical expansion imposed on the wall shock together with the strengthening effect on the concave wall.

Computed shock strengths are greater than those measured, because the critical shock is initially attenuated much more rapidly than is predicted by the model. This may occur in the instantaneous diffraction process, or more probably through interactions between the wall shock and the rapidly expanding flow behind it. These are shown to be short-range effects and are already insignificant at the first measuring station. Thus if the experimental shock strength at 1.86 diameters is used, the model predicts accurately the shock strength at 3.76 diameters.

The model is essentially a test of Chisnell's theory, which can therefore be applied to ducts with large abrupt increases in cross-section only when the wall shock is some distance from the entrance to the area change.

The work was carried out at the Central Electricity Research Laboratories and is published by permission of the Central Electricity Generating Board. The authors would like to thank Dr V. M. Morton for assisting with the numerical analysis and Professor A. G. Gaydon for many helpful discussions.

REFERENCES

- CHESTER, W. 1953 The propagation of shock waves in a channel of non-uniform width. *Quart. J. Mech. Appl. Math.* **6**, 440.
- CHESTER, W. 1954 The quasi-cylindrical shock tube. *Phil. Mag. Ser. 7*, **45**, 1293.
- CHISNELL, R. F. 1957 The motion of a shock wave in a channel with applications to cylindrical and spherical shock waves. *J. Fluid Mech.* **2**, 286.
- DAVIES, P. O. A. L. & GUY, T. B. 1971 Shock wave propagation in ducts with abrupt area expansions. *Symp. Internal Flows, Univ. Salford*, paper 30, p. D46.
- DECKKER, B. E. L. & GURURAJA, J. 1970 An investigation of shock wave behaviour in ducts with a gradual or sudden enlargement in cross-sectional area. *Fluid Mech. Conv., Univ. Glasgow*, paper 4, p. 27. (See also *Proc. Inst. Mech. Engrs* **184**, 3G.)
- NETTLETON, M. A. 1973 Shock attenuation in a gradual area change. *J. Fluid Mech.* **60**, 209.

- SKEWS, B. W. 1967 The shape of a diffracting shock wave. *J. Fluid Mech.* **29**, 297.
- SLOAN, S. A. & NETTLETON, M. A. 1975 A model for the axial decay of a shock wave in a large abrupt area change. *J. Fluid Mech.* **71**, 769.
- SMITH, C. E. 1966 The starting process of a hypersonic nozzle. *J. Fluid Mech.* **24**, 625.
- WHITHAM, G. B. 1957 A new approach to the problems of shock dynamics. Part 1. Two-dimensional problems. *J. Fluid Mech.* **2**, 145.
- WHITHAM, G. B. 1959 A new approach to the problems of shock dynamics. Part 2. Three-dimensional problems. *J. Fluid Mech.* **5**, 369.

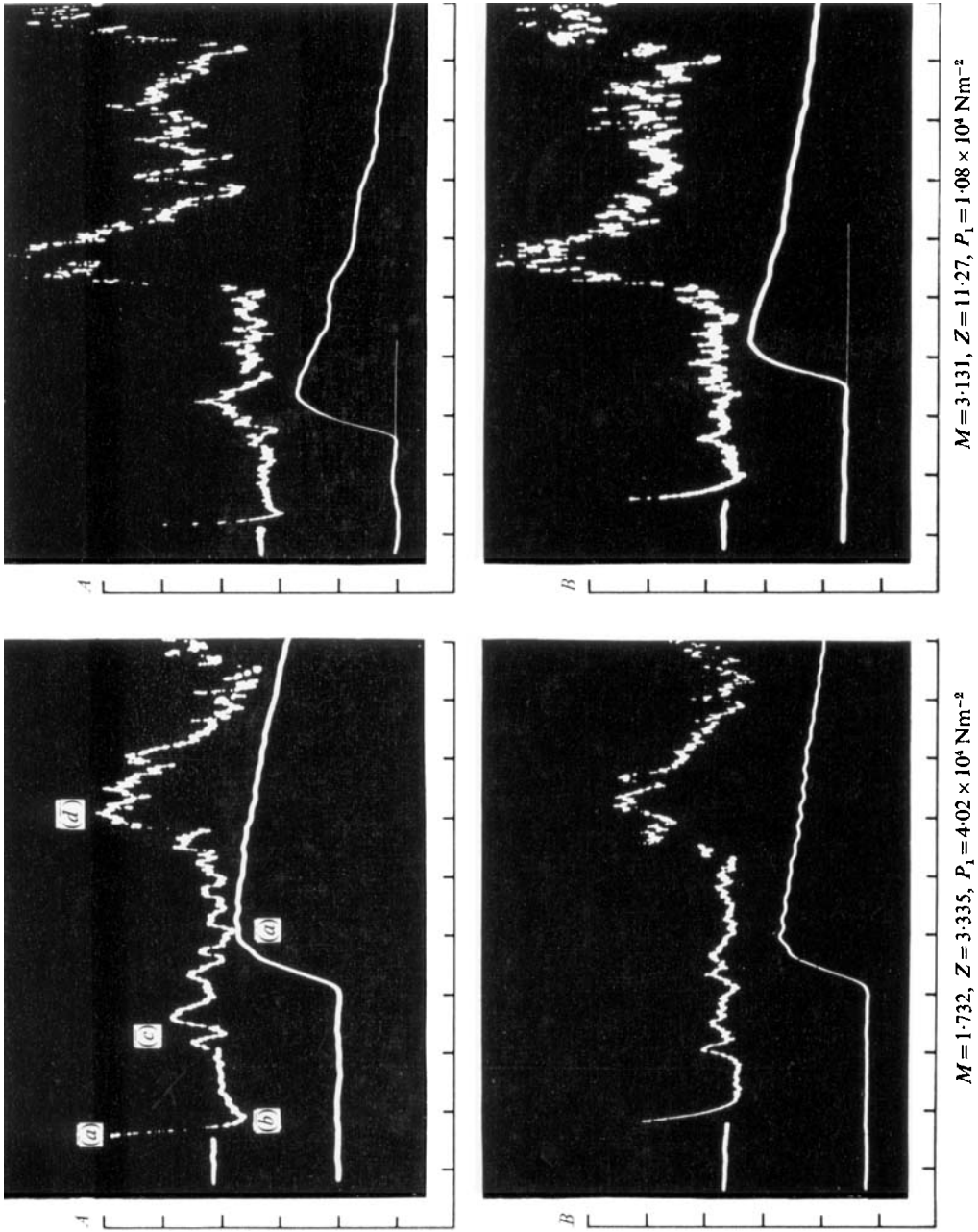


FIGURE 2. Typical pressure profiles. Upper traces, 1 ms div.^{-1} ; lower trace, $20 \mu\text{s div.}^{-1}$; A, $5.7 \times 10^3 \text{ Nm}^{-2} \text{ div.}^{-1}$; B, $5.3 \times 10^3 \text{ Nm}^{-2} \text{ div.}^{-1}$.